Available online at www.sciencedirect.com
ScienceDirect
Ceramics International 37 (2011) 3247–3251
CERAMICS INTERNATIONAL
www.elsevier.com/locate/ceramint

The effect of fluorine content on the mechanical properties of poly (ε-caprolactone)/nano-fluoridated hydroxyapatite scaffold for bone-tissue engineering

Narges Johari *, Mohammad Hossein Fathi, Mohammad Ali Golozar

Biomaterials Research Group, Department of Materials Engineering, Isfahan University of Technology, 8415683111, Isfahan, Iran

Received 20 February 2011; received in revised form 20 May 2011; accepted 22 May 2011
Available online 27 May 2011

Abstract

In this study, the effect of fluorine content on the mechanical properties of the novel poly (ε-caprolactone)/nano-fluoridated hydroxyapatite nanocomposite scaffolds was investigated. Poly (ε-caprolactone)/nano-fluoridated hydroxyapatite (PCL–FHA) scaffolds were produced by solvent casting/particulate leaching method. The fluoridated hydroxyapatite nanopowders had a chemical composition of $Ca_{10}(PO_4)_6OH_{2-x}F_x$ (where x values were selected equal to 0.5, 1, 1.5 and 2.0). Various weight percentages (10, 20, 30 and 40) of the FHA were added to the PCL. Sodium chloride (NaCl) particles having diameter of 300–500 μm were used as porogen. X-ray diffraction (XRD) and Fourier transform infrared spectroscopy (FT-IR) were used to identify the phase structure and functional groups of obtained scaffolds. Mechanical properties of the prepared scaffolds were also determined. Results showed that the compressive strength of scaffolds increases with decreasing the weight percent of fluorine in FHA.

Keywords: Poly (ε-caprolactone); Fluoridated hydroxyapatite nanopowders; Scaffold; Fluorine; Compressive strength

1. Introduction

Bone tissue, made of a collagen matrix containing hydroxyapatite nanocrystals, is a typical nanocomposite in view of its structure and composition. Because of the nanocomposite structure of the bone tissue, during the last years, the design of bone implants and bone scaffolds has been a major subject of consideration [1]. Human bone, especially in young people, has a high regenerative rate. Conversely, large defects, which may be caused by traumatic events, diseases or even natural ageing, require a proper support for the regenerative processes. The major aim of bone tissue engineering is to provide alternative solutions to promote the spontaneous bone regeneration processes. In particular, in order to assist the bone regeneration, proper scaffolds have been used as a template for cell interaction and new tissue ingrowth [2]. When bioactive ceramics, such as hydroxyapatite (HA), tricalcium phosphate (TCP) and bioglass, are hybridized with biodegradable polymers, such as polylactic acid (PLA), polyglycolic acid (PGA), polycaprolactone (PCL) and their copolymers, their mechanical properties, biological activity and osteoconductivity are improved [3]. There is no pure or composite of biodegradable polymer with bioactive inorganic phase that can effectively link to bone in vivo. PCL is a biodegradable polymer that has been attracted much interest because of its cost-efficiency, high toughness, and processability resulting from its relatively low melting temperature [4]. Most available scaffold fabrication methods are thermally induced phase separation (TIPS), solvent casting/particle leaching, solid free-form, microsphere sintering, and scaffold coating. Solvent casting method involves the dissolution of the polymer in an organic solvent, mixing with bioceramic, and casting the solution into a predefined three-dimensional mold. The advantage of this processing technique is the ease of fabrication without any specialized equipment to control the porosity and interconnectivity. However, in this method organic solvents are used and generally an isotropic structure is produced [5].

In the present study, fluoridated hydroxyapatite (FHA) was used as a bioactive bioceramic material to form a bone tissue scaffold. Fluorine exists as a trace element in the mineral phase of bone and tooth [6,7]. This is due to the formation of

* Corresponding author. Tel.: +98 311 3915708.
E-mail address: n.johari@ma.iut.ac.ir (N. Johari).

0272-8842/$36.00
doi:10.1016/j.ceramint.2011.05.119

fluoridated hydroxyapatite in teeth, which has a higher acid resistance than hydroxyapatite [8]. The fluoride ions are substituted for the hydroxide ions in the OH^- lattice positions [9]. Dissolution of hydroxyapatite is controlled by many factors such as: crystality, elemental stoichiometry ratio, and its chemical composition. One of the proper methods for decreasing the dissolution rate is substitution of OH^{-1} groups in hydroxyapatite by F^{-1} ions, which leads to the formation of fluorine-substituted hydroxyapatite. This ionic substitution causes an increase in crystallinity, a decrease in crystal strain, and an increase in thermal and chemical stability [10].

The mechanical properties also play a critical role in the bone fracture risk and strength [11,12]. The mechanical properties of bone are a function of factors such as the amount of mineralization, porosity, structural anisotropy and histology [13].

In this research, the effect of fluorine content on the mechanical properties of the novel PCL–FHA nanocmposite scaffolds was investigated and the optimum composition was determined.

2. Materials and method

2.1. Fabrication of PCL–FHA100 nanocomposite scaffolds

The FHA nanopowder was produced according to our previous work [14] using different amounts of fluoridation via mechanical alloying (MA) method. The FHA nanopowder was synthesized using a mixture of appropriate amounts of calcium hydroxide, phosphorous pentoxide, and calcium fluoride powders by 6 h of mechanical alloying at 300 rpm, using eight balls with a diameter of 20 mm, and the ball-to-powder weight ratio equal to 35:1. Crystallite size of FHA nanopowder was calculated using Williamson–Hall formula [14]. The selected amount for substitution of OH^{-1} by F^{-1} is indicated by the x value in the general formula of FHA ($Ca_{10}(PO_4)_6OH_{2-x}F_x$), where x values are equal to 0.5, 1, 1.5 and 2. The subsequent obtained nanopowders were named as FHA25, FAH50, FHA75 and FHA100, respectively. Various amounts (10, 20, 30 and 40 wt.%) of FHA were stirred vigorously in dichloromethane (DCM; CH_2Cl_2, Sigma–Aldrich, UK) for 1 h to disperse FHA uniformly. The commercially available PCL ($-[(CH_2)_5COO]_n$, Mw = 70,000–90,000, Sigma–Aldrich, UK) was then added to solution and stirred for 2 h to dissolve completely. Sodium chloride (NaCl) particles having diameter of 300–500 μm were then incorporated into the suspension (NaCl/(PCL + FHA) = 60, 70 and 80% (w/w), were named P1, P2, and P3, respectively). The dispersion was finally cast into a Teflon mold (d = 8 mm, h = 18 mm). The ratio of PCL:DCM was 10% (w/v) [15]. The samples were air-dried for 48 h to allow the solvent to evaporate. They were then vacuum-dried at room temperature for 48 h to remove any remaining solvent. Subsequently, the samples were immersed in deionized water for a period of 72 h, and the water was changed at an approximately every 6 h at room temperature in order to leach the salt particulates out.

2.2. Phase structure analyses

Phase structure analyses of PCL–FHA scaffolds with different types of FHA (FAH25, FHA50, FHA75 and FHA100) were carried out by X-ray diffractometer (XRD, Philips Xpert) using Ni filtered CuKα ($\lambda_{CuK\alpha}$ = 0.154186 nm, radiation at 40 kV and 30 mA) over the 2θ range of 10–60°.

2.3. Investigation of functional groups and structure of scaffolds

The functional groups of the obtained scaffolds with different FHA were analyzed by Fourier transform infrared spectroscopy (FT-IR, Tensor 27, Bruker) in a mid-IR spectrum range, within the range of 400–4000 cm^{-1}.

2.4. Morphological study

Morphologies of pore structure were studied using SEM (Phillips XL 30: Eindhoven, The Netherlands).

2.5. Porosity measurement

Using a specific gravity bottle, based on Archimedes' Principle [16], the porosity of scaffolds was measured and calculated as follows:

$$\text{porosity}(\%) = \frac{(w_2 - w_3 - w_s)/\rho_e}{(w_1 - w_3)/\rho_e} \times 100 \quad (1)$$

where w_1 is the weight of bottle filled with ethanol; w_2, the weight of bottle containing ethanol and scaffold; w_3, the weight of bottle taken out of ethanol-saturated scaffold; w_S, is the weight of the scaffold; and ρ_e is, the density of ethanol.

2.6. Mechanical testing

Compression tests were performed on the prepared porous scaffolds (d = 8 mm, h = 10 mm) according to ASTM, D3410/D3410M [17]. For this purpose, a Zwick materialprüfung 1446 tension/compression machine was used. The crosshead speed was 2 mm/min in the ambient conditions. The obtained stress–strain curves were used to determine the compression properties. The compressive strength was determined from the maximum stress recorded. Three specimens were tested for each condition and the results were reported in the form of mean values.

The main shortcoming of the compression tests is the low modulus with elastic collapse stress. This phenomenon is due to the morphological properties and the pore structure of the scaffolds [18].

3. Results and discussion

Phase analysis results of the PCL–FHA nanocomposites with different types of FHA (FHA25, FHA50, FHA75 and FHA100) are shown in Fig. 1. Typical PCL and FHA peaks

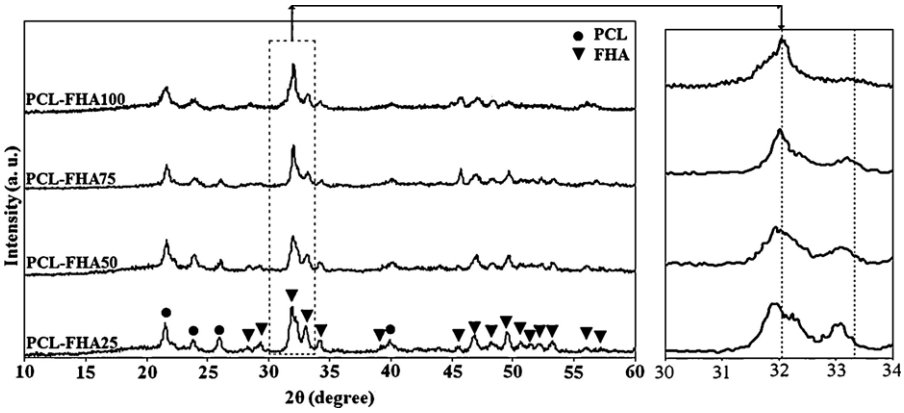

Fig. 1. XRD patterns of produced PCL–FHA scaffolds with different types of FHA.

(according to XRD JCPDS data file No. 15-0876) were observed in all prepared nanocomposites. Similar PCL peaks have been reported by Kim et al. [3]. Comparing the XRD patterns of PCL–FHA100 and PCL–FHA25 scaffolds, it is observed that some sets of FHA100 characteristic peaks have gradually shifted to the right. The slight shift of characteristic peaks to the right, which has also been observed by other researchers [19,20], is believed to be related to the decrease of the *a*-axis length of the hexagonal HA crystal lattice, due to a lower ionic radii of F^{-1} compared with OH^{-1}. This can cause distortion in the crystal lattice by incorporation of fluorine ions instead of hydroxyl groups in the apatite structure [10].

Fig. 2 shows the FT-IR spectroscopy results of PCL/FHA nanocomposites. As seen here, characteristic structural bands of both FHA and PCL are observed for all PCL/FHA nanocomposites.

The C=O, C–O, and C=H bands corresponding to PCL and the P–O and O–H bands are attributed to FHA [21]. All the characteristic group contributions identified to be consistent with PCL structure, including: (1) $-(CH_2)_4-$skeletal group within the regions of 3000–2850 cm^{-1} and 1250–1450 cm^{-1}; (2) C=O bonds in the region centered at 1750 cm^{-1}; and (3) C–O groups within the region of 1150–1250 cm^{-1}. A strong absorption centered at 1750 cm^{-1} is indicative of an aliphatic ester [22].

The characteristic peaks of PO_4^{3-} group are observed at 961 and 471 cm^{-1}. A major peak of phosphate group is noticed in the region of 1100 and 1000 cm^{-1} [23]. In fact, it is seen that the PO_3^{4-} absorbance emerges within the ranges of 950–1100 and 550–620 cm^{-1} [21].

It has been reported in the previous researches [19,24], that the spectrum of the hydroxyapatite sample shows clear bands corresponding to structural hydroxyl groups at 630 and 3572 cm^{-1}, suggesting the incorporation of fluoride ions into the apatite lattice for FHA100 sample. The 3572 cm^{-1} is attributed to a weakly hydrogen bond and 630 cm^{-1} is assigned to strong hydrogen bond [24]. It is believed that these two vibrations at hydroxyapatite are due to OH^{-1} immersed in an infinite chain of OH^{-1} but this chain is interrupted by F^{-1} in FHA100. As the fluoride ion incorporate into the apatite lattice, the bands assigned to the F···OH (740 cm^{-1}) appear and the bands assigned to the structural OH^{-1} disappear [25].

Fig. 3 shows the typical SEM micrographs of the PCL–FHA100 porous scaffolds with various NaCl/(PCL + FHA100) ratios. Respectively, micrographs of the produced scaffolds with P1, P2 and P3 ratios, are depicted in Fig. 3(a–c). The pore

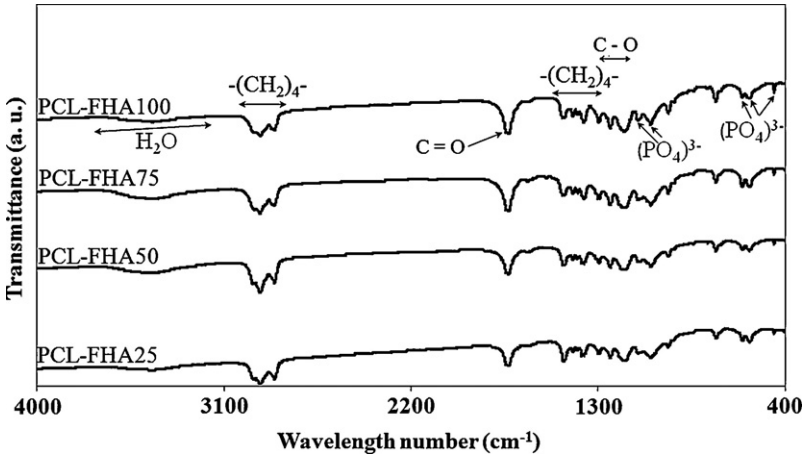

Fig. 2. FTIR spectra of produced PCL–FHA100 scaffolds with different types of FHA100.

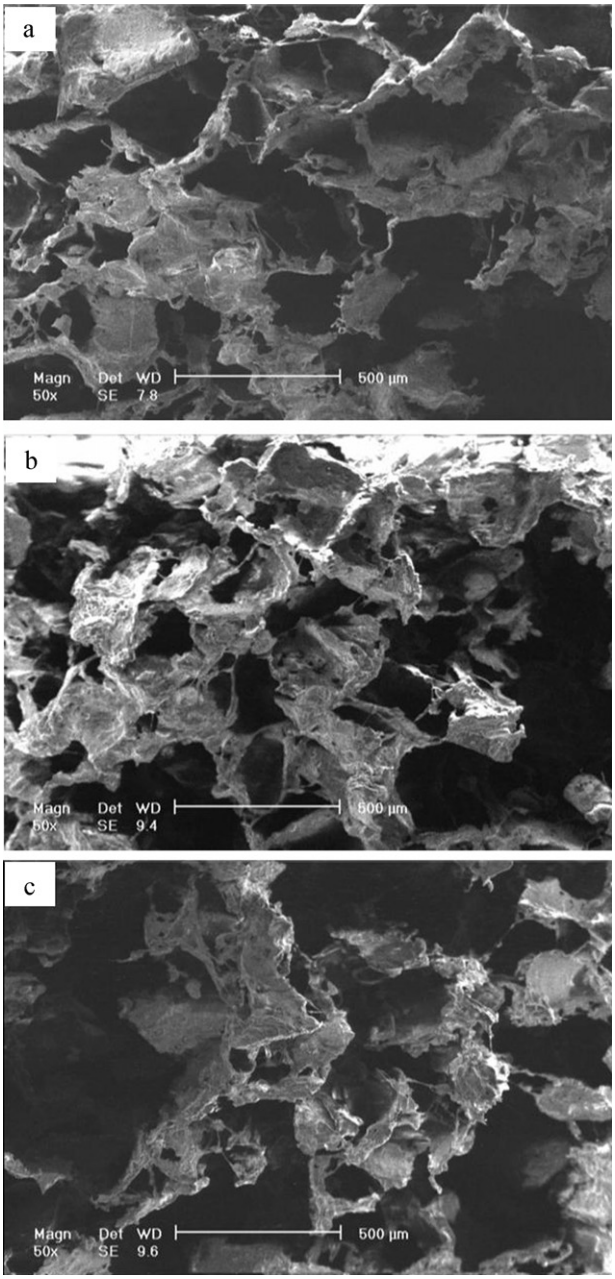

Fig. 3. SEM micrographs of PCL–FHA100 with (a) P1, (b) P2 and (c) P3 ratios.

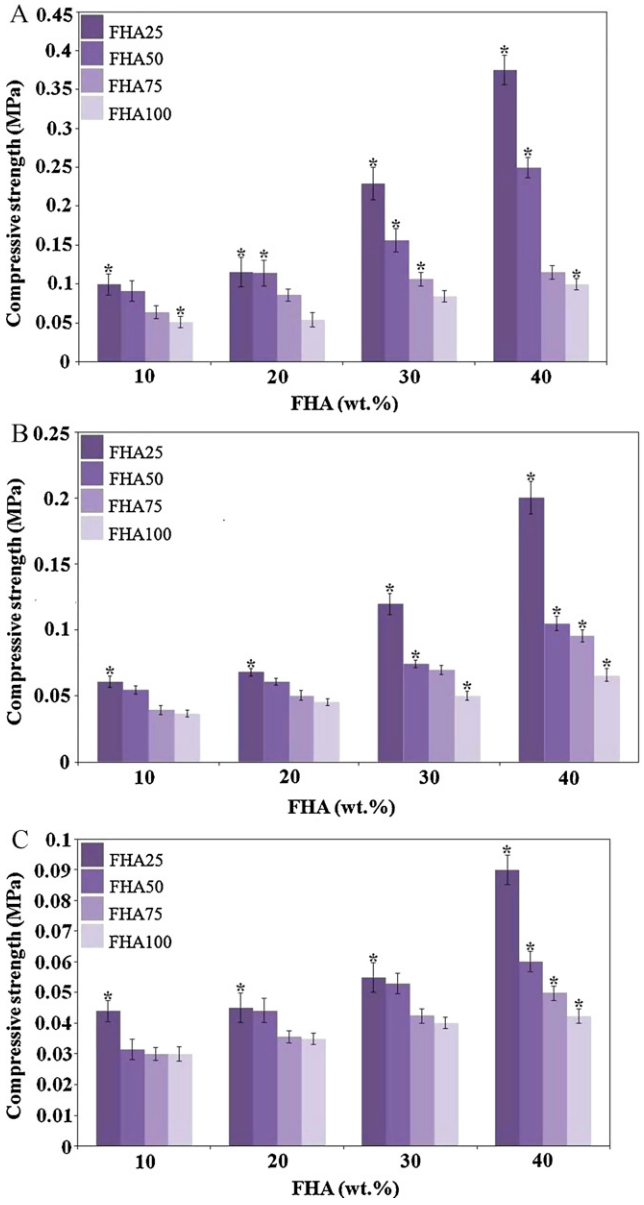

Fig. 4. Effect of fluorine content on compressive strength of the porous PCL–FHA scaffolds with different ratios of NaCl/(PCL + FHA): (a) P1, (b) P2 and (c) P3 ($n = 3$, values are mean ± SD, $^*p < 0.05$).

shape of polymer/FHA100 scaffold could be seen in this figure. An open pore structure was observed. The SEM morphologies show that with increasing the NaCl/(PCL + FHA) ratio, the porosity of scaffolds is also increased.

Mechanical properties of the porous scaffolds used in tissue engineering are of particular importance, since they are closely linked to shape-persistency and durability in practical operations and applications [16]. Table 1 shows the percentage of scaffolds porosity measured.

Compressive strength has universally been used to evaluate the mechanical properties of ceramics materials. Fig. 4 shows the mean values of compressive strength of produced porous PCL–FHA scaffolds with varying levels of fluorine substitution in FHA. Fig. 4(a–c) shows the effect of NaCl/(PCL + FHA) ratio on the scaffolds compressive strength. The compressive strength of scaffolds increases with decreasing the weight ratio of fluorine in FHA. As is seen, the PCL–FHA100 and the PCL–FHA25 scaffolds show the minimum and the maximum compressive strength respectively. It has been shown that the crystallite size of FHA powders increase as a result of increasing fluorine content [25]. Obtained results in this work also showed a significant decrease of lattice parameter and crystallite size of FHA having lower content of fluorine. These results are in a good agreement with slight shift of characteristic peaks in Fig. 1 as well as the work published by others [19]. Mechanical properties of synthetic calcium phosphates decrease significantly with increasing amorphous phase, microporosity and grain size. High crystallinity, low porosity

Table 1
Obtained porosity percents by Archimedes' principle for produced scaffolds ($n = 3$).

Sample	NaCl/(PCL + FHA)	Porosity percent
PCL-10nFHA100	P1	64 ± 6
	P2	80 ± 5
	P3	90 ± 4
PCL-20nFHA100	P1	63 ± 4
	P2	75 ± 3
	P3	85 ± 5
PCL-30nFHA100	P1	60 ± 5
	P2	73 ± 4
	P3	83 ± 3
PCL-40nFHA100	P1	58 ± 2
	P2	70 ± 4
	P3	80 ± 4

and small grain size tend to obtain higher stiffness, higher compressive and tensile strengths, and greater fracture toughness [5].

The maximum compressive strength of the scaffold was observed for PCL-40FHA25 nanocomposite scaffolds and NaCl/(PCL + FHA) ratio equal to 60% (w/w) (P1). It has also been reported by Ghassemieh [26] that addition of bioceramic to polymer, could improve the mechanical properties of scaffolds. The porosity of the nanocomposite scaffold has a noticeable effect on its compressive strength [15]. The scaffolds exhibit minimal compressive strength, with the maximal porosity.

4. Conclusion

PCL–FHA nanocomposite scaffolds were produced by solvent casting/particulate leaching method. 10, 20, 30 and 40 wt.% FHA (FHA25, FHA50, FHA75 and FHA100) nanopowders were added to nanocomposite scaffolds. Characteristic structural bands of both FHA and PCL were observed for all PCL/FHA ratios. In the produced scaffolds, the porosity increased with an increase in the porogen (NaCl particles). The compressive strength of scaffolds increased with decreasing the weight percent of fluorine in FHA. The maximum compressive strength of the scaffold was obtained for PCL-40FHA25 nanocomposite scaffolds and NaCl/(PCL + FHA) ratio equal to 60% (w/w) (P1).

References

[1] I. Kotela, J. Podporska, E. Soltysiak, K.J. Konsztowicz, M. Blazewicz, Polymer nanocomposites for bone tissue substitutes, Ceram. Int. 35 (2009) 2475–2480.
[2] V. Karageorgiou, D. Kaplan, Review porosity of 3D biomaterial scaffolds and osteogenesis, Biomaterials 26 (2005) 5474–5491.
[3] H.W. Kim, E.J. Lee, H.E. Kim, V. Salih, J.C. Knowles, Effect of fluoridation of hydroxyapatite in hydroxyapatite–polycaprolactone composites on osteoblast activity, Biomaterials 26 (2005) 4395–4404.
[4] S. Lauren, G. Selcuk, W. Xuejun, G. Milind, S. Wei, Fabrication of three-dimensional polycaprolactone/hydroxyapatite tissue scaffolds and osteoblast-scaffold interactions in vitro, Biomaterials 28 (2007) 5291–5297.
[5] K. Rezwana, Q.Z. Chena, J.J. Blakera, A.R. Boccaccini, Biodegradable and bioactive porous polymer/inorganic composite scaffolds for bone tissue engineering, Biomaterials 27 (2006) 3413–3431.
[6] T.S.B. Narasaraju, D.E. Phebe, Some physico-chemical aspects of hydroxylapatite, J. Mater. Sci. 31 (1996) 1–21.
[7] M. Okazaki, H. Tohda, T. Yanagisawa, M. Taira, J. Takahashi, Differences in solubility of two types of heterogeneous fluoridated hydroxyapatites, Biomaterials 19 (1998) 611–616.
[8] J.E. Tyler, Comparitive dissolution studies on human enamel and fluorapatite, Caries Res. 4 (1970) 23–30.
[9] J. Lucas, Fluorine in the natural environment, J. Fluorine Chem. 41 (1988) 1–8.
[10] Y. Chen, X. Miao, Thermal and chemical stability of fluorohydroxyapatite ceramics with different fluorine contents, Biomaterials 26 (2005) 1205–1210.
[11] P. Chavassieux, E. Seeman, P.D. Delmas, Insights into material and structural basis of bone fragility from diseases associated with fractures: how determinants of the biomechanical properties of bone are compromised by disease, Endocr. Rev. 28 (2007) 151–164.
[12] J. Currey, Incompatible mechanical properties in compact bone, J. Theor. Biol. 231 (2004) 569–580.
[13] J. Currey, Bones: Structure and Mechanics, Princeton University Press, Princeton, New Jersey, 2002.
[14] M.H. Fathi, E. Mohammadi Zahrani, Mechanical alloying synthesis and bioactivity evaluation of nanocrystalline fluoridated hydroxyapatite, J. Cryst. Growth. 311 (2009) 1392–1403.
[15] J. Wei, F. Chen, J.W. Shin, H. Hong, C. Dai, J. Su, C. Liu, Preparation and characterization of bioactive mesoporous wollastonite–polycaprolactone composite scaffold, Biomaterials 30 (2009) 1080–1088.
[16] Y. Wan, H. Wu, X. Cao, S. Dalai, Compressive mechanical properties and biodegradability of porous poly (caprolactone)/chitosan scaffolds, Polym. Degrad. Stab. 93 (2008) 1736–1741.
[17] ASTM, Standard test method for compressive properties of polymer matrix composite materials with unsupported gage section by shear loading, ASTM, 1997, D3410/D3410M.
[18] Y. Ung, S.S. Kim, H.K. Young, S.H. Kim, B.S. Kim, S. Kim, Y.C. Cha, H.K. Soo, A poly (lactic acid)/calcium metaphosphate composite for bone tissue engineering, Biomaterials 26 (2005) 6314–6322.
[19] E. Mohammadi Zahrani, M.H. Fathi, The effect of high-energy ball milling parameters on the preparation and characterization of fluorapatite nanocrystalline powder, Ceram. Int. 35 (2009) 2311–2323.
[20] B.H. Yoon, H.W. Kim, S.H. Lee, C.J. Bae, Y.H. Koh, Y.M. Kong, H.E. Kim, Stability and cellular responses to fluorapatite–collagen composites, Biomaterials 26 (2005) 2957–2963.
[21] F. Yang, S.K. Both, X. Yang, X.F. Walboomers, J.A. Jansen, Development of an electrospun nano-apatite/PCL composite membrane for GTR/GBR application, Acta Biomater. 5 (2009) 3295–3304.
[22] R. Cristescu, A. Doraiswamy, G. Socol, S. Grigorescu, E. Axente, D. Mihaiescu, A. Moldovan, R.J. Narayan, I. Stamatin, I.N. Mihailescu, B.J. Chisholm, D.B. Chrisey, Polycaprolactone biopolymer thin films obtained by matrix assisted pulsed laser evaporation, Appl. Surf. Sci. 253 (2007) 6476–6479.
[23] M.H. Fathi, E. Mohammadi Zahrani, Fabrication and characterization of fluoridated hydroxyapatite nanopowders via mechanical alloying, J. Alloys Compd. 475 (2009) 408–414.
[24] C.Y. Ooi, M. Hamdi, S. Ramesh, Properties of hydroxyapatite produced by annealing of bovine bone, Ceram. Int. 33 (2007) 1171–1177.
[25] L.M. Rodriguez-Lorenzo, J.N. Hart, K.A. Gross, Influence of fluorine in the synthesis of apatites. Synthesis of solid solutions of hydroxy-fluorapatite, Biomaterials 24 (2003) 3777–3785.
[26] E. Ghassemieh, Morphology and compression behaviour of biodegradable scaffolds produced by the sintering process, J. Eng. Med. 222 (2008) 1247–1262.